PICTS Analysis of Extended Defects in Heavily Irradiated Silicon

David Menichelli, Emilio Borchi, Zheng Li, and Mara Bruzzi

***Abstract*—We report the results of an experimental study on radiation-induced defects in silicon p^+n diodes irradiated with 1-MeV neutrons up to a fluence of 2.3×10^{15} cm^{-2}. Heavily irradiated silicon diodes have been studied by means of Photo Induced Current Transient Spectroscopy (PICTS) technique using a variable filling time. For every filling time, a dominant broad and structured peak has been found in the temperature range 200–300 K. Such a broad peak cannot be accounted for by considering isolated point defects, being consistent with a quasi-continuous distribution of deep levels inside the bandgap. In addition, it is observed that the spectral lineshape tends to broaden as the filling time is increased. The details of the lineshape modifications depend strongly on the irradiation fluence of the sample, in such a way that they cannot be explained only in terms of emissions from noninteracting electron states. Thus we suggest that the investigated broad peak should, at least in part, be generated by emission from extended defects, also known as clusters.**

***Index Terms*—DLTS, PICTS, TSC, extended defects, irradiated silicon, silicon detectors.**

I. Introduction

SILICON junction detectors are widely used in a variety of application fields characterized by a hostile radiation environment. In particular, silicon devices are planned to be used as forward tracker detectors both in ATLAS (A Toroidal Lhc ApparatuS) [1] and Compact Muon Solenoid (CMS) [2] experiments at the large Hadron collider (LHC) at CERN. The very high radiation levels foreseen in these experiments are expected to seriously deteriorate the electrical properties of these devices. This has stimulated an ever-increasing research effort on the radiation damage in silicon.

It is well known that fast neutrons are able to produce displacement cascades in such a way that the primary state of damage involves extended regions of the semiconductor [3]–[7]. The thermally activated rearrangement of the lattice defects should result in both isolated point defects as well as defect clusters [8], [9]. The clustering of vacancy-interstitial pairs, after irradiation with ions and electrons, has also been directly observed by electron microscopy [10], [11].

Lattice disorder in heavily irradiated silicon detectors is frequently studied by Photo Induced Current Transient Spectroscopy (PICTS) [12]–[14], also known as I-DLTS (Current-Deep Level Transient Spectroscopy). This technique is based on the measurements of current transients due to carrier emission from deep levels. PICTS allows one to determine the microscopic electronic properties of the defects (activation energy E and capture cross section σ) and to obtain some information about the defect concentration N_t.

The electrical activity of a point defect differs from that of a cluster for two reasons. First, when many point defects group together inside a small region, their energy levels split to form a continuous density of states. Second, when many carriers are trapped inside a cluster, a Coulomb barrier grows around the extended defect, inhibiting further trapping. In [15], it was argued that, inside depleted regions, it could be difficult to distinguish isolated defect and cluster emission, because the electric field of the depleted region should be dominant with respect to the cluster Coulomb field. This observation does not take into account the phenomenon of level splitting. In fact, more recently, an abnormal broadening of PICTS peaks has been interpreted as the signature for defect clusters [16]–[18], even if a clear demonstration that broad peaks in PICTS spectra of irradiated silicon arise from clusters is presently lacking. In addition, it has been shown that Coulomb barrier effects are not second order ones in many situations, such as plastically deformed silicon [19], [20] and precipitates in silicon [21], [22].

It has been argued that, defect cluster emission may be identified by directly measuring several DLTS spectra for different filling pulse times t_p and looking for spectrum shape modifications [20], [23]. According to the standard DLTS theory [14], the lineshape of a single deep level should not change when changing the filling time. Let us consider for instance an electron trap. The single-level current transient $I(t,T)$ at fixed temperature T is given by

$$I(t,T) = I(\infty,t) + \frac{1}{2} qAwn_t(t_p)e_e(T)\exp(-te_e). \quad (1)$$

Here q is the electron charge, A the sample area and w the depletion depth. $n_t(t_p)$ is the density of the states filled by an excitation pulse with duration t_p. $I(\infty,T)$ is the reverse current of the junction at the temperature T. $e_e = \gamma_e T^2 \sigma \exp(-E/kT)$ is the electron emission coefficient, k being the Boltzmann constant and γ_e a constant depending on the material. The DLTS spectrum $S(T)$ is defined as

$$S(T) = I(t_1,T) - I(t_2,T) \quad (2)$$

where t_1 and t_2 are the DLTS sampling times. The filling of the trap at constant temperature is ruled by the differential equation

$$\dot{n}_t = c_e(N_t - n_t) - e_e n_t \quad (3)$$

Manuscript received November 24, 2001; revised April 12, 2002 and June 14, 2002.

D. Menichelli, E. Borchi, and M. Bruzzi are with Dipartimento di Energetica di Firenze, 50139 Florence (Italy) and also with INFM Firenze, Sesto Fiorentino (FI), Italy (e-mail: bruzzi@fi.infn.it).

Z. Li is with Brookhaven National Laboratory, Upton, NY 11973 USA.

Digital Object Identifier 10.1109/TNS.2002.803881

where N_t is the total trap concentration. $c_e = \sigma v n$ is the electron capture coefficient, v being the electron thermal velocity and n the free carrier concentration. Since n is fixed by the excitation ($n \sim 10^9$ cm^{-3} in our experiments), the occupation evolution is

$$n_t(t) = n_{\rm tsat}\left[1 - \exp\left(-\frac{t}{t_{\rm sat}}\right)\right]. \quad (4)$$

Here $n_{\rm tsat} = N_t c_e/(c_e + e_e)$ and $t_{\rm sat} = 1/(c_e + e_e)$. Note that at the spectrum peak temperature carrier emission is far from negligible; thus $n_t \ll N_t$, and PICTS cannot be used to directly evaluate trap concentration. A more reliable technique to measure trap concentration is thermally stimulated currents (TSC) spectroscopy.

The capture coefficient c_e exhibits a weak dependence on temperature, through $v \sim \sqrt{T}$. Thus, the variations of $n_{\rm tsat}$ and $t_{\rm sat}$ with temperature are ruled by $e_e(T)$. It follows that both $n_{\rm tsat}$ and $t_{\rm sat}$ decrease with T. In addition, at a fixed T, they grow with E, due to the diminished emission rate. For a single level, the variations of $n_t(t_p)$ with temperature are always considered as a second-order effect. Thus, when changing the filling time, the lineshape is expected to merely change its amplitude, until t_p is long enough to ensure trap saturation.

If the emissions from many single levels overlap, the total spectral shape may change with t_p if some levels saturate, while others do not. If, due to particular experimental conditions, this effect can be ruled out, the shape of a spectrum due to a sum of point defect contributions is not expected to depend on t_p. Anyway, it has been shown that an anomalous line broadening can be due to the setup of a Coulomb barrier around a cluster [20]. This phenomenon leads to nonexponential current transients and to a t_p-dependent lineshape.

II. Samples and Experimental Setup

We studied a set of p$^+$ /n/n$^+$ detectors, produced by boron implantation on phosphorous doped silicon at the Brookhaven National Laboratory (Upton, NY). The depth of the implants is about 200 nm, and their doping level about 10^{16} cm^{-3}. These diodes have a nominal resistivity $\rho = 400-500\,\Omega\cdot$cm, an active area $A = 0.25$ cm^2 and a thickness $W = 260 - 280\,\mu$m. A circular window (radius 1 mm) in the metallization was etched on the front side to allow for optical excitation. The samples were irradiated with fast neutrons at UMass Lowell (up to a neutron fluence of $\Phi = 7.9\times10^{13}$ n/cm^2), and at the ATOMKI Institute of Nuclear Research of Debrecen, Hungary ($\Phi = 4.7\times10^{14}$, 9.3×10^{14}, 2.3×10^{15} n/cm^2). All the fluences have been normalized to 1-MeV neutron. The measurements have been carried out two years after the irradiation. During this time, the samples were kept at room temperature. The effective doping concentration $N_{\rm eff}$ can be deduced from initial resistivity, irradiation fluence and annealing time, using the results reported in [24]. For our samples we obtain the results of Table I, where effective doping concentrations $N_{\rm eff}$, depletion depths w at $V_{\rm rev} = 5$ V and full depletion voltages V_d are reported.

PICTS experiments were performed in the temperature range 30–300 K. The experimental setup is depicted in Fig. 1. The sample excitation is provided by a light-emitting diode (LED) with wavelength $\lambda = 940$ nm, rise time 80 ns and fall time 180 ns. The maximum optical power incident over the sample optical windows is on the order of 1 mW. The LED is driven by a pulse generator (Systron Donner 110D), which allows one to vary the excitation pulse duration t_p starting from 500 ns. A photodiode is used to monitor the LED activity. The current transients generated by the pulsed light across the sample are measured using a custom readout circuit. It converts the current into voltage, ensuring adequate values of transresistance ($r = 0.5 \div 1\times10^6$ V/A), input resistance ($R_{\rm in} = 2.2$ kΩ) and bandwidth (BWD $= 1$ MHz). The readout circuit has three stages, constituted by a current–voltage converter followed by two voltage amplifiers. An operational amplifier ensuring a fast recovering from saturation (Analog OP467G) was used to construct each stage. Thus the readout circuit can be used to clamp the photocurrent peak, which is superimposed on the current emitted by deep levels, in order to avoid saturation of the oscilloscope input circuit. The whole readout circuit recovers its linear behavior from deep saturation in about 3 μs. The oscilloscope (Tektronix TD520D, 500 MHz) samples the transients to produce the PICTS spectrum; we adopted the sampling times

TABLE I
Effective Doping Concentration $N_{\rm eff}$, FullDepletion Voltage V_d and Depletion Depth w Calculated for the Samples Used in the Paper. The Depletion Depths are Relative to the Reverse Bias $V_{\rm rev} = 5$ V

Fluence ϕ (10^{14} x cm^{-2})	$N_{\rm eff}$ (10^{13} x cm^{-3})	$V_{\rm d}$ (kV)	w (μm)
0.2	1.7	0.90	19.7
0.34	1.8	0.95	19.1
0.53	1.9	1.01	18.5
0.79	2.1	1.10	17.8
4.7	4.4	2.36	12.1
9.3	7.2	3.85	9.5
23	15.1	8.28	6.5

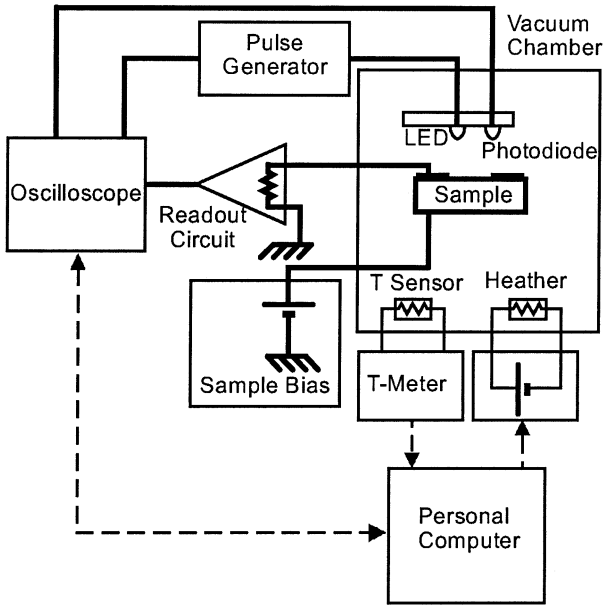

Fig. 1. PICTS experimental setup. Thick line: fast analog signals; thin line: slow analog signals; dashed line: digital signals.

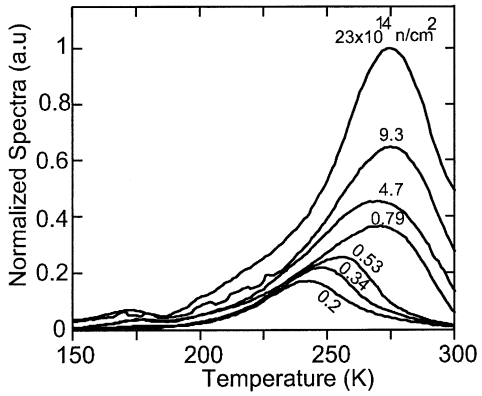

Fig. 2. Normalized PICTS spectra obtained from samples irradiated with different neutron fluences, taken with $t_p = 50$ μs. The neutron fluence (expressed as $\Phi/10^{14}$ n/cm^2) is reported close to each curve.

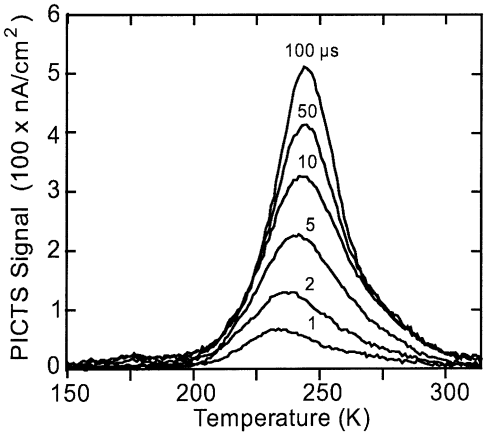

Fig. 3. PICTS spectra of the sample irradiated up to $\Phi = 2 \times 10^{13}$ n/cm^2, using different excitation pulse duration t_p. The filling times, expressed in μs, are reported above each curve.

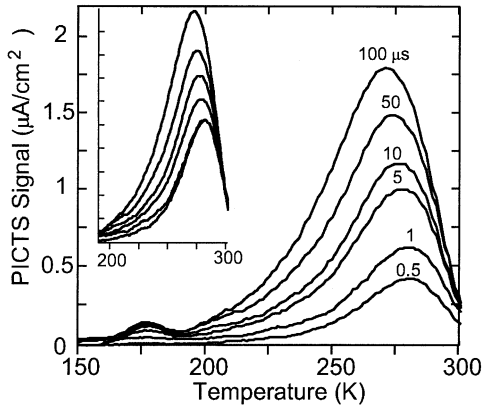

Fig. 4. PICTS spectra of the sample irradiated up to $\Phi = 7.9 \times 10^{13}$ n/cm^2, obtained using different excitation pulse duration t_p. The filling times, expressed in μs, are reported above each curve. In order to evidence spectral shape modification, each curve is multiplied by a constant, as shown in the inset.

$t_1 = 100$ μs and $t_2 = 450$ μs. A constant heating rate (less than 0.07 K/s), slow enough not to affect the shape of the spectrum, was adopted. The bias applied to the sample was $V_{\rm rev} = 5$ V. The bias and the upper limit of the explored temperature range are limited by the growth of the reverse current.

III. Experimental Results and Discussion

The dominant features of the PICTS spectra occur between 150 and 300 K. Three additional peaks of reduced amplitude are located near 50, 80, and 110 K. They are commonly observed in PICTS spectra of irradiated silicon [17] (the latter being usually related to the point defects C_iC_s and VO_i). Due to their sharp shape, they are not believed to have a relation with extended defects; thus they have not been considered in this study.

The general shape of the spectra generated by our samples in the range $T = 150 - 300$ K is shown in Fig. 2. For each sample the pulse intensity was adjusted in order to maximize the signal-to-noise ratio. Thus the spectra generated by the different samples have been normalized to the relative light intensity, as detected by the photodiode, in order to get a significant comparison. As a common feature, a very broad and distorted peak can be observed between 200 and 300 K. New high-temperature components arise as the irradiation fluence is increased. The total defect concentration is related to irradiation fluence and annealing time. The PICTS peak amplitude grows with defect concentration, but this technique is not reliable for a quantitative estimate of N_t, as discussed in Section I. However, a qualitative indication of the relative defect concentration in the different samples can be obtained by dividing the spectra amplitudes of Fig. 1 by the depletion depth of the various samples. It has been noted [17] that this broad peak cannot be fitted using few isolated deep levels, and that the broadening is not observed in samples irradiated with gamma rays (which are not effective in creating extended damaged regions). The conclusion was that this spectral feature may be related to defect clusters. Similarly it has been argued [18] that a quasi-continuous distribution of deep levels may be suitable to explain simultaneously PICTS and TSC spectra of similar samples. According to [18], the number of different deep levels contributing to the PICTS spectrum grows with fluence. The main features of the spectrum corresponding to the less irradiated sample can be accounted for by few deep levels near 0.36 eV, with a cross section $\sigma = 10^{-15}$–10^{-16} cm^2. As the fluence rises to 7.9×10^{13} cm^{-2} the contribution from a distribution of levels between 0.4 and 0.45 eV ($\sigma = 10^{-15} - 10^{-14}$ cm^2) broaden the peak toward higher temperatures. In the highest fluence range a group of levels in the range 0.47–0.49 eV ($\sigma = 10^{-15} - 10^{-14}$ cm^2) becomes dominant. These three groups of levels might be related to C_iO_i, double vacancy and, perhaps, V_2O, respectively. Note that clusters at room temperature are believed to be composed mainly of vacancy aggregates, such as double vacancy and, possibly, higher order aggregates [25]. The interaction between oxygen, carbon and double-vacancy clusters has been invoked to account for radiation damage in high resistivity n-type silicon after proton irradiation [26]–[28].

The effect of changing the filling time in the range $t_p = 1 - 100$ μs can be observed in Figs. 3–5. The behavior of the lineshape in these three cases is representative of the whole set of samples. For filling times longer than 100 μs the lineshape does not undergo further modifications, while the peak amplitude tends to saturate. Fig. 3 refers to the sample irradiated up to $\Phi = 2 \times 10^{13}$ n/cm^2. The lineshape is strongly asymmetric, and

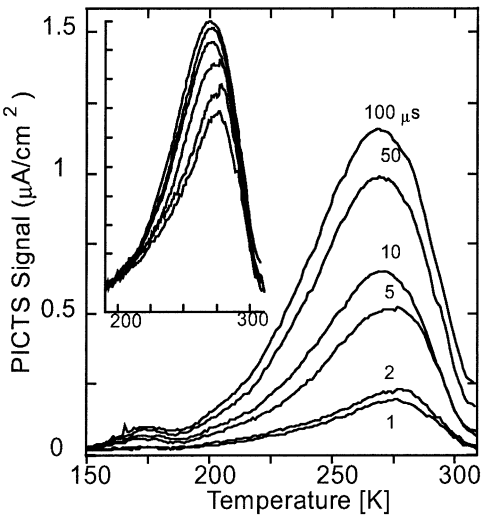

Fig. 5. Normalized PICTS spectra of the sample irradiated up to $\Phi = 4.7 \times 10^{14}$ n/cm^2, using different excitation pulse duration t_p. The filling times, expressed in μs, are reported close to each curve. Inset like indicated in Fig. 4.

presents a high temperature shoulder between 260 and 300 K. The amplitude of the shoulder saturates if $t_p > 10\,\mu$s. The main component is peaked near 240 K and saturates for $t_p > 100\,\mu$s. The peak position shifts toward higher temperature only before shoulder saturation. We can conclude that this shifting is due to the growing of shoulder components, and there is no need to invoke the existence of a Coulomb barrier around defects.

The as-measured spectra of the sample irradiated up to $\Phi = 0.79 \times 10^{14}$ n/cm^2 are shown in Fig. 4. These spectra are peaked close to 275 K, while the spectra of Fig. 3 were peaked at about 250 K. This is because new levels have been created by the increased irradiation. A normalized plot is shown in the insets: in order to evidence lineshape modification, each curve has been multiplied by an arbitrary constant, to align the different high-T sides. The lineshape modification is very different from that of Fig. 3. The peak broadens toward lower temperatures as t_p is increased, while the peak position shifts about 10 K toward the low temperature range. The low-T sides of the peaks remain almost parallel. Signal saturation is observed for $t_p > 100\,\mu$s, but spectra deformation starts as $t_p > 1\,\mu$s. Thus the lineshape broadening cannot be easily explained in terms of point defects.

Finally, the spectra of the sample irradiated up to $\Phi = 4.7 \times 10^{14}$ n/cm^2 are shown in Fig. 5. Similarly to the case of Fig. 4, the peak broadens toward lower temperatures, and the peak position is shifted by about 10 K as t_p is increased. However, the slope of the low-T side now rises with t_p, while signal saturation is observed for $t_p > 200\,\mu$s. Even in this case lineshape broadening initiates as t_p exceeds few microseconds.

According to [18], for the two most irradiated samples, we expect the dominant spectral features to be related to deep levels with $E > 0.4$ eV. For these levels, in the temperature range $T = 200-300$ K, using (4), we find $t_{\rm sat} = 10^{-5}-10^{-2}$ s. The lineshape amplitude saturates when $t_p > 100\,\mu$s, as expected from our estimate, and the whole broad dominant peak grows continuously as t_p changes from 1 μs to 100 μs. However, line shape modifications occur at filling times much shorter than the saturation value, and the dominant spectral features might then be reasonably assigned to emissions from defect clusters surrounded by a Coulomb barrier.

Note that (1) is obtained under the assumptions that: 1) the defect concentration N_t is much smaller than the bulk doping concentration N_d and 2) the depletion region extends almost totally through the bulk. If N_t is not much smaller than N_d the depletion depth experiences strong fluctuations during emission and capture phenomena, leading to a non- exponential transient and lineshape modifications [14], [29]. In our samples the depletion depth is mainly determined by the concentration of deep levels, thus a not truly exponential transient is expected. However, we obtain from (3) that, as long as $t_p < 50\,\mu$s, the ratio of filled traps is $n_t/N_t < 0.01$ for all the levels in the range 0.35-0.49 eV. It follows that, within this t_p range, trapping and emission phenomena cannot produce relevant depletion depth fluctuations. Since in our experiments the lineshape changes as soon as t_p exceeds few μs, this observation cannot be accounted for by depletion depth modulations.

Had N_t approached the implant doping concentration, then the depletion region would extend through the implant, leading to further lineshape distortion effects. However, even in the case of the most irradiated sample considered in this work, the implant doping concentration (about 10^{16} cm^{-3}) is much higher than $N_{\rm eff}$. In turn, the depletion depth on the implant side (about 80 nm at $V_{\rm rev} = 5$ V) remains much smaller than the depletion depth on the bulk side x_d. Thus, this phenomenon cannot introduce substantial lineshape modifications.

IV. Conclusion

PICTS measurements, with filling time varying in the range $t_p = 1 - 500\,\mu$s, have been carried out on heavily irradiated silicon p$^+$ /n/n$^+$ diodes. As the irradiation fluence exceeds the value $\Phi = 7.9 \times 10^{13}$ n/cm^2, the PICTS spectra exhibit a broad and "distorted" peak in the temperature range $T = 200-300$ K. This spectral feature is commonly reported in literature; it has been associated with quasi-continuous distributions of deep levels inside the bandgap [18] related, at least in part, to double vacancies. The peak amplitude saturates if $t_p > 100\,\mu$s, but the line shape changes with filling time even if t_p is much lower than the saturation value ($t_p > 1\,\mu$s). These observations cannot be accounted for in terms of isolated point defects. Similar lineshape modifications have been observed during the study of processing-induced extended defects in silicon, such as dislocations and precipitates [21]. Thus, we suggest that the dominant spectral features might be related to emissions from defect clusters.

In principle, it is possible to distinguish extended defects from point defects by plotting the peak amplitude versus filling time: a nonlinear (logarithmic) behavior far from saturation should indicate the existence of a Coulomb barrier [19]. Further information, such as Coulomb barrier height and density of states, can be deduced by spectra fitting [20]. Unfortunately, in our case, due to the large number of localized states in the range $E = 0.4 - 0.5$ eV, and to the fact that at least two different defects (related to V_2^- and, probably, to V_2O) are involved in clustering, it is difficult to carry out quantitative estimates. The

study of samples irradiated with particles which are not effective in generating displacement cascades (such as gamma rays), should allow one to isolate the point defect features from the cluster features in PICTS spectra; this type of analysis has been scheduled by the authors. In addition, some preliminary studies indicate that the $n_t(t_p)$ dependency on temperature, at least in some cases, may be simply not a second order effect. Further investigations about this issue are needed to draw quantitative conclusions.

ACKNOWLEDGMENT

The authors thank Prof. W. Schröter, from Universität Göttingen, for helpful discussions on extended defects in semiconductors. They are grateful to Dr. J. Molnar and Dr. A. Fenyvesi of the ATOMKI Institute of Nuclear Research of Debrecen, Hungary, for having performed part of the samples irradiation. Finally, we thank K. Waggoner for his help in editing the manuscript.

REFERENCES

[1] "The ATLAS Technical Proposal," ATLAS Collaboration, Geneva, Switzerland, CERN/LHCC/94–43, LHCC/P2, 1994.

[2] "The Compact Muon Solenoid Technical Proposal," CMS Collaboration, Geneva, Switzerland, CERN/LHCC/94–38, 1994.

[3] V. A. J. van Lint and E. G. Wikner, "Correlation of radiation types with radiation effects," *IEEE Trans. Nucl. Sci.*, vol. NS-10, pp. 80–87, Jan. 1963.

[4] H. J. Stein, "Defects in silicon: concepts and correlations," in *Radiation Effects in Semiconductors*, J. W. Corbett and G. D. Watkins, Eds. New York: Gordon & Breach, 1970, pp. 125–140.

[5] V. J. A. van Lint, R. E. Leadon, and J. F. Colwell, "Energy dependence of displacement effects in semiconductors," *IEEE Trans. Nucl. Sci.*, vol. 19, pp. 181–185, Dec. 1972.

[6] M. J. Caturla, T. Diaz de la Rubia, and G. H. Gilmer, "Disordering and defect production in Silicon by keV ion irradiation studied by molecular dynamics," *Nucl. Instrum. Meth. B*, vol. 106, pp. 1–8, 1995.

[7] R. S. Averback and T. Diaz de la Rubia, "Displacement damage in irradiated metals and semiconductors," *Solid State Phys.*, vol. 51, pp. 281–401, 1998.

[8] A. J. van Lint, "The physics of radiation damage in particle detectors," *Nucl. Instrum. Meth. A*, vol. 253, pp. 453–459, 1987.

[9] T. Diaz de la Rubia, N. Soneda, M. J. Caturla, and E. A. Alonso, "Defect production and annealing kinetics in elemental metals and semiconductors," *J. Nucl. Mat.*, vol. 251, pp. 13–33, Nov. 1997.

[10] L. M. Howe and M. H. Rainville, "Features of collision cascades in Silicon as determined by transmission electron microscopy," *Nucl. Instrum. Meth.*, pt. 1, vol. 182, pp. 143–151, May 1981.

[11] L. Fedina, A. Gutakovskii, A. Aseev, J. Van Landuyt, and J. Vanhellemont, "Extended defects formation in Si crystals, by clustering of intrinsic point defects studied by in-situ electron irradiation in a HREM," *Phys. Stat. Sol. A*, vol. 171, no. 1, pp. 147–157, 1999.

[12] D. V. Lang, "Deep-level transient spectroscopy: A new method to characterize traps in semiconductors," *J. Appl. Phys.*, vol. 45, no. 7, pp. 3023–3032, 1974.

[13] C. H. Hurtes, M. Boulou, A. Mitonneau, and D. Bois, "Deep-level spectroscopy in high-resistivity materials," *Appl. Phys. Lett.*, vol. 32, no. 12, pp. 821–823, 1978.

[14] P. Blood and J. W. Orton, *The Electrical Characterization of Semiconductors: Majority Carriers and Electron States*. London, U.K.: Academic, 1992.

[15] B. L. Gregory, S. S. Naik, and W. G. Oldham, "Neutron produced trapping centers in junction field effect transistors," *IEEE Trans. Nucl. Sci.*, vol. NS-18, pp. 50–59, Dec. 1971.

[16] D. Cavalcoli, A. Cavallini, and E. Gombia, "Energy levels associated with extended defects in plastically deformed n-type Silicon," *J. Phys. III France*, vol. 7, no. 7, pp. 1399–1409, 1997.

[17] V. Eremin, A. Ivanov, E. Verbitskaya, Z. Li, and S. U. Pandey, "Analysis of divacancy related traps induced by proton, neutron and Gamma radiation in high resistività Silicon detectors," *Nucl. Instrum. Meth. A*, vol. 426, no. 1, pp. 120–125, 1999.

[18] D. Menichelli, S. Pirollo, and Z. Li, "A detailed microscopic analysis of deep levels in heavily irradiated-medium resistivity Silicon detectors," *IEEE Trans. Nucl. Sci.*, vol. 47, pp. 446–451, Apr. 2000.

[19] P. Omling, E. R. Weber, L. Montelius, H. Alexander, and J. Michel, "Electrical properties of dislocations and point defects in plastically deformed Silicon," *Phys. Rev. B*, vol. 32, no. 10, pp. 6571–6581.

[20] W. Schröter, J. Kronewitz, U. Gnauert, and M. Seibt, "Bandlike and localized states at extended defects in Silicon," *Phys. Rev. B*, vol. 52, no. 19, pp. 13 726–13 729, 1995.

[21] F. Riedel and W. Schröter, "Electrical and structural properties of nanoscale $NiSi_2$ precipitates in Silicon," *Phys. Rev. B*, vol. 62, no. 11, pp. 7150–7155, 2000.

[22] M. Seibt, H. Hedemann, A. A. Istratov, F. Riedel, A. Sattler, and W. Schröter, "Structural and electrical properties of metal silicide precipitates in Silicon," *Phys. Stat. Sol. A*, vol. 171, no. 1, pp. 301–310, 1999.

[23] H. Hedemann and W. Schröter, "Deep-level transient-spectroscopy for localized states at extended defects in semiconductors," *J. Phys. III France*, vol. 7, no. 7, pp. 1389–1398, 1997.

[24] G. Lindström, M. Moll, and E. Fretwurst, "Radiation hardness of Silicon detectors – A challange from high-energy physics," *Nucl. Instrum. Meth. Phys. Res. A*, vol. 426, no. 1, pp. 1–15, 1999.

[25] Y. Shi, D. X. Shen, F. M. Wu, and K. J. Cheng, "A numerical study of cluster center formation in neutron-irradiated Silicon," *J. Appl. Phys.*, vol. 67, no. 2, pp. 1116–1118, 1990.

[26] Z. Li and H. W. Kraner, "Studies of frequency dependent CV characteristics of neutron irradiated p^+/n^- Silicon detectors," *IEEE Trans. Nucl. Sci.*, vol. 38, pp. 244–250, Apr. 1991.

[27] E. Borchi, M. Bruzzi, S. Pirollo, and S. Sciortino, "Temperature and frequency dependence of the capacitance of heavily irradiated Silicon diodes," *Solid-State Electron.*, vol. 60, no. 11, pp. 2093–2096, 1998.

[28] M. Kuhnke, E. Fretwurst, and G. Lindstroem, "The annealing of interstitial Carbon in high resistivity n-type Silicon after proton irradiation," *Nucl. Instrum. Meth. Phys. Res. A*, vol. 485, no. 1–2, pp. 140–145, June 2002.

[29] A. C. Wang and C. T. Sah, "Determination of trapped charge emission rates from nonexponential capacitance transients due to high trap densitied in semiconductors," *J. Appl. Phys.*, vol. 55, no. 2, pp. 565–570, 1984.